ELSEVIER

Journal of Hazardous Materials 53 (1997) 195–211

JOURNAL OF HAZARDOUS MATERIALS

Theoretical and experimental investigation of combustion to detonation transition in chemically active gas mixtures in closed vessels

N.N. Smirnov *, I.I. Panfilov, M.V. Tyurnikov, A.G. Berdyuguin, V.R. Dushin, Yu.P. Presnyakov

Department of Mechanics and Mathematics, Moscow State University, 119899 Moscow, Russian Federation

Received 12 December 1995; accepted 26 April 1996

Abstract

This paper presents the results of numerical and experimental investigations of the process of deflagration to detonation transition. It is shown that both regimes of combustion to detonation transition and regimes including deflagration waves lagging behind the shock waves are possible. Several types of flow patterns of deflagration to detonation transitions are determined theoretically and experimentally. Stability of one- and two-dimensional detonation waves is investigated. It is shown that one-dimensional pulsations in the symmetrical case with free boundaries cause strong transverse pulsations. © 1997 Published by Elsevier Science B.V.

Keywords: Chemically active gas mixture; Combustion; Detonation transition

1. Introduction

There are many experiments [1–3] that show deflagration in a combustible gas mixture contained in a tube accelerating towards detonation near the closed end of the tube. It is shown experimentally that detonation waves can originate in the vicinity of the flame zone [1,3] very close to the primary shock wave [10] and any place in between [2,11,12]. Many authors [4–9,13] have numerically modelled the onset of detonation in such systems. These authors considered one-dimensional models and simplified one-stage reactions. Molecular transfer effects were neglected [5–7], with the focus of the study

* Corresponding author. Department of Mechanics and Mathematics, Moscow State University, 119899 Moscow, Russia. Tel: 7-095-9391190. Fax: 7-095-9394995.

PII S0304-3894(96)01801-8

being directed towards understanding how ignition is caused by initial non-uniformities of temperature and concentration of species. The presence of such non-uniformities could spontaneously lead to initiation of detonation in initially quiescent gas.

This work [13] shows that under some circumstances exothermic chemical reactions in an Euler fluid could support the convergence of characteristics, leading to the formation of an internal shock detonation behind the leading shock wave. This occurred for both a piston supported flow and behind a reflected shock wave. Other works [8,9] have focused on modelling detonation initiation in a viscous, thermoconductive gas. The various stages of combustion from initiation to reaction completion for the case when a heat flux is applied to a half-infinite region filled with an active mixture were analyzed in detail [8]. The calculational results agreed with the experimental observation and helped to define a detailed mechanism for the process. The present paper investigates how the presence of a 2-step kinetic mechanism, the difference in characteristic times for the induction step and for the exothermic step, and the igniting conditions affect the initiation process and deflagration to detonation transition.

2. Mathematical model.

Here we model evolution of an initially quiescent combustible mixture inside a tube, bounded by flat, rigid, non-catalytic walls. Our study is based on the standard mathematical model of nonstationary flow of a chemically reactive, viscous, thermoconductive gas. The governing system of equations is:

$$\frac{\partial \rho}{\partial t} + \operatorname{div} \rho \boldsymbol{u} = 0, \tag{1}$$

$$\frac{\partial \rho \delta}{\partial t} + \operatorname{div} \rho \delta \boldsymbol{u} = \operatorname{div}(\rho D \operatorname{grad} \delta) - \dot{w}_{\delta}, \tag{2}$$

$$\frac{\partial \rho Y_1}{\partial t} + \operatorname{div} \rho Y_1 \boldsymbol{u} = \operatorname{div}(\rho D \operatorname{grad} Y_1) - \dot{w}, \tag{3}$$

$$\frac{\partial \rho \boldsymbol{u}}{\partial t} + \operatorname{div} \rho \boldsymbol{u} \cdot \boldsymbol{u} = -\operatorname{grad} p + \operatorname{div} J, \tag{4}$$

$$\frac{\partial \rho h}{\partial t} + \operatorname{div} \rho h \boldsymbol{u} = \Delta H \dot{w} + \operatorname{div}\left(J \boldsymbol{u} + \lambda \operatorname{grad} T + \rho T D \sum_{j=1}^{2} c_{pj} \operatorname{grad} Y_j \right) + \frac{\partial p}{\partial t}, \tag{5}$$

where: ρ, u, p, T are density, velocity, pressure and temperature of gas mixture, respectively; Y_i, m_i, c_{pi} $(i = 1, 2)$ are mass concentration, molar mass, specific heat at constant pressure of the ith component; $h = \sum_{i=1}^{2} c_{pi} Y_i T + u^2/2$ is the complete mixture enthalpy per mass unit; μ, λ, D are the transfer coefficients (viscosity, thermoconductivity and diffusion, respectively); ΔH is the specific heat of combustion; J is a viscous stress tensor with its components $\|\tau^{ik}\|$, $\operatorname{div} J$ is a vector with components $\sum_{i=1}^{3} \nabla_i \tau^{ik}$, $k = 1,2,3$; $\operatorname{div} \rho \boldsymbol{u} \cdot \boldsymbol{u}$ is a vector with components $\sum_{i=1}^{3} \nabla_i \rho v^k v^i$, $k = 1,2,3$.

Parameter δ characterizes the part of the induction period left.

The chemical kinetics is modelled by a two-stage mechanism: the induction period when δ changes from 1 to 0 with the rate $\dot{w}_\delta = K_\delta \rho \exp(-E_\delta/RT)$ and the exothermic stage with the rate of reaction $\dot{w} = K\rho Y_1 p\chi(-\delta)\exp(-E_a/RT)$, where E_a, E_δ are the activation energies, and $\chi(z)$ is a Heavyside function.

Assuming that each component of the combustible mixture has a molar mass m_i and obeys an ideal gas equation of state:

$$p = \rho RT \sum_{j=1}^{2} \frac{Y_j}{m_j}, \tag{6}$$

and also $\sum_{j=1}^{2} Y_j = 1$, closes the system of equations (1)–(5).

3. One-dimensional model

To begin with we regard a one-dimensional flat flow of viscous heat-conducting chemically reacting gas mixture boarded with flat solid non-catalytic walls at $x = 0$ and $x = L$. One-dimensional models are very useful in mechanics because on the one hand there exist many exact analytical solutions of one-dimensional problems that provide good tests for numeric investigations, and on the other hand the most important characteristic features of one-dimensional flow can be observed in much more sophisticated multidimensional flows.

It is more convenient to study the system (1)–(5) in Lagrangian mass coordinates $q(x, t) = \int_0^x \rho(r, t)\,dr$. The coordinates (q, t) are particularly useful in the zone where there are large gradients of density (shock waves).

We rewrite the equations in dimensionless variables and define an appropriate set of dimensionless parameters. The characteristic parameters used in the scaling are:

$$\rho_1, T_1, m_1, c_{p1}, c_{v1}, M = \int_0^L \rho(r, t)\,dr = \text{const}, \mu_1, a_1 = \frac{\sqrt{\gamma_1 RT_1}}{m_1}, t_a = L/a_1$$

where $\gamma_1 = c_{p1}/c_{v1}$.

It should be remarked that there exist several characteristic process times: an acoustic time $t_a = L/a_1$, a conduction time $t_c = L^2(\lambda_1/\rho_1 c_{p1})^{-1}$, the induction time $t_i = (K_\delta \rho)^{-1} \exp(E_\delta/RT)$, and the characteristic time for energy release $t_e = (K\rho)^{-1} \exp(E_a/RT)$. The scaled dependent variables used in our equations are the following: pressure p, density ρ, velocity u, temperature T.

Using (q, t) as independent variables, the system of Eqs. (1)–(6) can be written in dimensionless form as:

$$\frac{\partial U}{\partial t} + \frac{\partial G(U)}{\partial q} = J(U), \tag{7}$$

$$p = \rho T \left(Y + \frac{m_1}{m_2}(1 - Y) \right) / \gamma_1, \tag{8}$$

where $G(U) = F(U) + \nu(U)\,\partial f(U)/\partial q, Y = Y_1$, and vector-functions U, F, f, J and matrix ν are described in Ref. [15]. All the variables in the system (7) and (8) are dimensionless. The similarity parameters of the system are the following:

$$\mathrm{Re} = \frac{\rho_1 a_1 L}{\mu_1};\ \mathrm{Pr} = \frac{\mu_1 c_{p1}}{\lambda_1};\ \mathrm{Sc} = \frac{\mu_1}{\rho_1 D_1};\ \theta_\delta = \frac{E_\delta}{R_{\mathrm{un}} T_1};$$

$$\theta_a = \frac{E_a}{R_{\mathrm{un}} T_1};\ \frac{\Delta H}{c_{p1} T_1};\ \frac{c_{p2}}{c_{p1}};\ \frac{m_2}{m_1};\ \mathrm{Da}_i = \frac{t_a}{t_{il}};\ \mathrm{Da}_e = \frac{t_a}{t_{el}}. \tag{9}$$

The initial and boundary conditions in the dimensionless form for the case of forced ignition are as follows:

$$t = 0\colon\ 0 \le q \le q_0\colon\ u = 0;\ \rho = 1;\ T = r_T;\ Y_1 = 0;\ \delta = 0;$$

$$q_0 < q \le 1\colon\ u = 0;\ \rho = 1;\ T = 1;\ Y_1 = 1;\ \delta = 1. \tag{10}$$

$$q = 0,\ q = 1\colon\ u = 0;\ \frac{\partial Y_1}{\partial q} = 0;\ \frac{\partial \delta}{\partial q} = 0;\ \frac{\partial T}{\partial q} = 0. \tag{11}$$

4. Results of numerical modelling

The numerical solution of the system (7) and (8) was obtained using a fraction step, time split method that just advanced the hydrodynamics and then the chemistry [16].

The results are displayed using nondimensional variables:

$$X = \frac{x}{L};\ \bar{t} = \frac{t c_1}{L};\ \bar{p} = \frac{p}{\rho_1 c_1^2};\ \bar{T} = \frac{T}{T_1};\ \bar{u} = \frac{u}{c_1};\ \rho = \frac{\rho}{\rho_1},$$

where the 1 index relates to the parameters of the initial unreacted combustible mixture. The values of the parameters are as follows:

$$\gamma_1 = 1.4;\ \frac{c_{p2}}{c_{p1}} = 1.2;\ \frac{m_1}{m_2} = 0.8;\ \mathrm{Re}_1 = 10^6;\ \mathrm{Pr}_1 = \mathrm{Sc}_1 = 0.72;\ \frac{\Delta H}{c_{p1} T_1} = 10;$$

$$\mathrm{Da}_i \exp\theta_\delta = \mathrm{Da}_e \exp\theta_e = 10^9.$$

The calculations show that the flow structure differs greatly depending on the activation energies E_a, E_δ. For relatively high values $\theta_a = 34$, $\theta_\delta = 34$ the calculation shows that after an initial transient, a structure forms that includes a shock wave, a region of a constant flow which is then followed by a combustion wave. A transition to detonation does not occur. The speed of the leading shock stabilizes at $U_{Yb} = 1.9$ and the speed of the flame front becomes $U_{fp} = 1.1$. The speed of the flame front is subsonic both relative to the unburnt mixture (combustion rate $U_f = 0.1$) and relative to the reaction products ($U_f^* = 1.05$). Lowering the activation energy to $\theta_a = 17$, $\theta_\delta = 17$ leads almost instantly to the development of a strong detonation wave that is coincident with the point of the shock formed by the forced ignition condition. This wave eventually slows down to the Chapman–Jouguet speed. At the intermediate value of activation energy $\theta_a = 21$, $\theta_\delta = 21$ (Fig. 1), a combustion wave is initially formed that

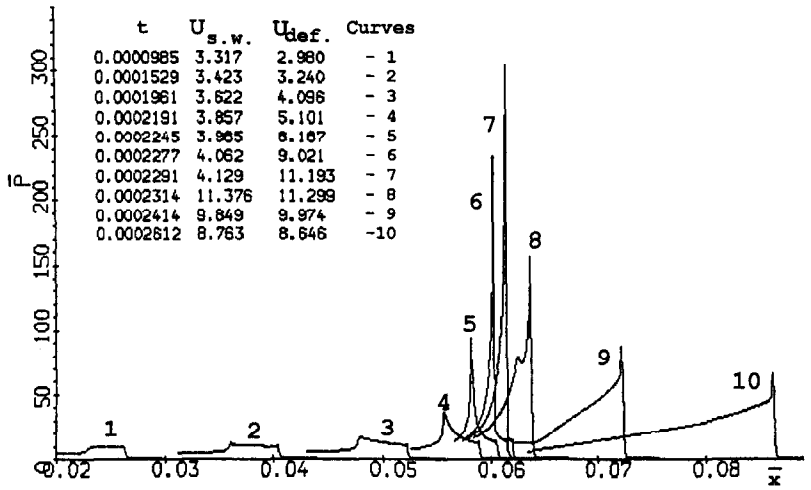

Fig. 1. Calculated pressure profiles in gas mixtures for deflagration to detonation transition for different times. Activation energy parameters $\theta_a = 8.4$, $\theta_\delta = 24$. Times and corresponding shock wave (U_{sw}) and flame (U_{def}) velocities for the numbered curves are given by the table in the Figure.

lags the shock formed by the forced ignition condition. As time passes, the pressure in the area between the shock wave and the combustion front increases, with the maximal rate of increase found immediately ahead of the flame front. The reaction zone accelerates rapidly and as it does so its length decreases. The detonation wave forms in the compressed gas in the vicinity of the flame front. The detonation then moves towards the leading shock wave. After the detonation interacts with the leading shock, an overdriven detonation wave is formed that spreads through the fresh mixture. Its initial speed is $U_D \sim 10$, which exceeds the velocity of Chapman–Jouguet detonation $U_{cj} = 7.2$. Gradually its intensity falls, and the detonation approaches the Chapman–Jouguet state. Thus, when the ignition of the combustible mixture is forced at the closed tube end, we can obtain either a detonation or combustion wave depending on the activation energies of the mixture.

Two different deflagration to detonation transition scenarios can occur. One of them is shown in Fig. 1. The other scenario is shown in Fig. 2 and corresponds to a transition where the detonation forms on a contact surface that forms in the zone of compressed gas between the leading shock and flame front. This contact surface may form as a result of a shock collision in front of the flame zone, when the ignited zone of gas is located at some distance from the closed end of a tube and a weak shock wave reflected from the wall ($x = 0$) overtakes the leading shock. Fig. 2 shows the pressure and temperature profiles at a number of different times. The sharp rise of temperature (dashed curve) up to $T \sim 10$ takes place in the flame zone. A contact surface, clearly seen on the temperature profiles, exists between the flame zone and the leading shock for times $t \geq t_3$. The zone between the leading shock and the contact surface has the higher temperature. Thus, the induction period in this zone is less than between the flame front and the contact surface. The first explosion takes place in the layer of gas that has been

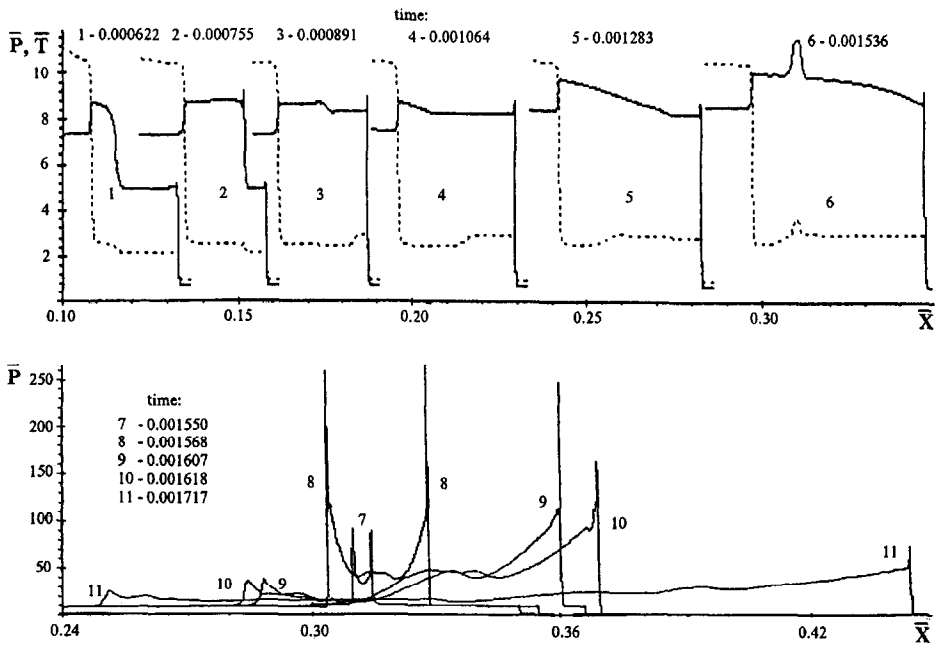

Fig. 2. Calculated pressure and temperature profiles at different times for the case of deflagration to detonation transition, when two weak shock waves precede the deflagration wave (curves 1, 2), a contact surface forms as a result of shock collision (curves 3, 4 and 5) that gives birth to two detonation waves propagating in opposite directions (curves 6, 7 and 8), and one of those waves becomes a schock wave on entering the combusted gas (curves 9, 10 and 11).

at the higher temperature for the longest time, i.e. in the gas layer very close to the contact surface. This leads to the birth of two detonation waves propagating in opposite directions. The intensity of the retonation (reverse detonation) wave falls on entering the reaction products after. The principal forward detonation wave propagates towards the leading shock. After it interacts with the leading shock, an overdriven detonation is transmitted into the 'cold' mixture. This wave decelerates down to the Chapman–Jouguet speed.

Our numerical experiments show us that the kinetic parameters and the initial ignition state determine where the contact surface formed is located between the reaction front and the leading shock at the moment of explosion. Thus, the place of detonation formation may be located either in the vicinity of the flame front or close to the leading shock.

5. Two-dimensional model.

Though one-dimensional models are very helpful in describing detonation phenomena, there exist some peculiarities such as transverse pulsations, wave curvature and side expansion in the explosion with free boundaries, that can be described only with the help

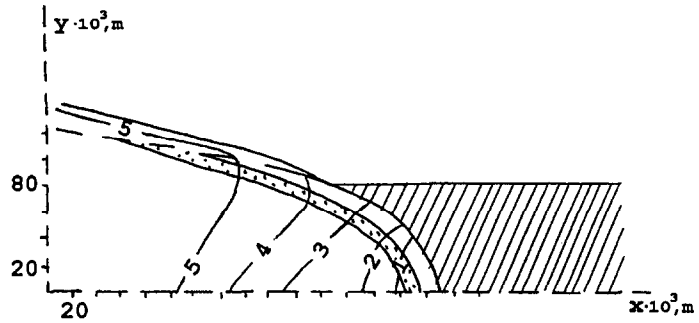

Fig. 3. A typical flow structure for a self-sustaining detonation when the induction zone is much larger than the reaction zone. Figures by the curves correspond to the following pressure ratios p/p_0: 1 – 68.0; 2 – 23.0; 3 – 20.0; 4 – 17.0; 5 – 15.0.

of multi-dimensional models. In this part of the paper we regard the problem of detonation wave propagation in the layer of finite thickness with free boundaries. The plane detonation wave formed in the channel with fixed boundaries at time $t = 0$ enters the layer of the same gas mixture with free boundaries. Owing to the fact that we regard the detonation process, the mathematical model (1)–(5) can be simplified by taking out of consideration effects of molecular diffusion, viscosity and thermal conductivity. The

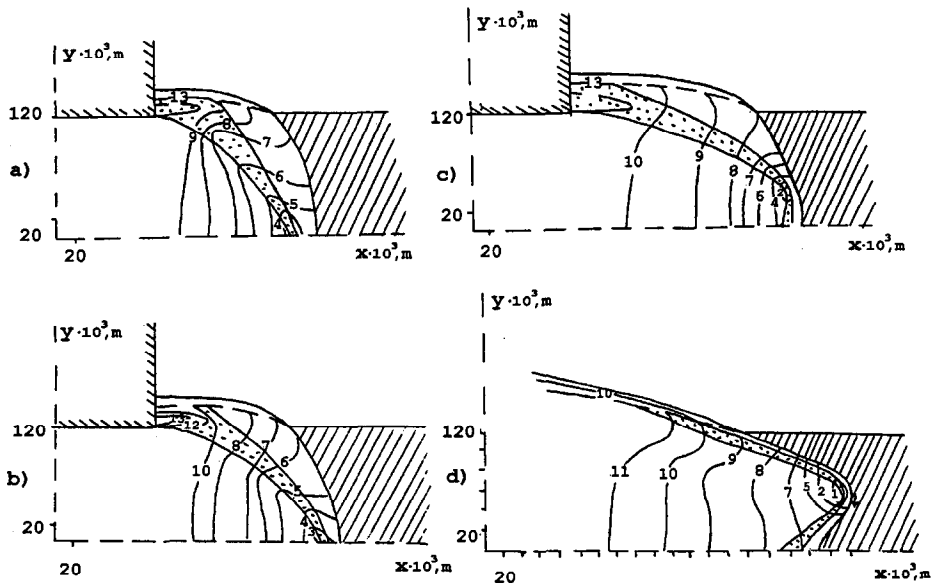

Fig. 4. A typical flow structure for a self-sustaining detonation when the induction zone is much larger than the reaction zone. Figures by the curves correspond to the following pressure ratios p/p_0: 1 – 68.0; 2 – 52.0; 3 – 48.0; 4 – 42.0; 5 – 35.0; 6 – 32.0; 7 – 26.0; 8 – 22.0; 9 – 18.0; 10 – 16.0; 11 – 13.0; 12 – 6.0; 13 – 3.0 (a – $t = 6.2\times10^{-5}$ s, b – $t = 6.2\times10^{-5}$ s; c – $t = 7.0\times10^{-5}$ s; d – $t = 8.0\times10^{-5}$ s).

system of equations was solved by use of a modified Godunov's scheme [15]. This scheme gives sufficient accuracy in solving the problems of multi-dimensional flows of chemically reacting gas mixtures [14,16]. The calculations were carried out for the following values of kinetic parameters: $n_1 = 2; n_2 = 1; n_3 = 2; n_4 = 2$. Two groups of kinetic parameters $E_a, E_\alpha, k, k_\alpha$ were chosen to form two types of self-sustaining wave flow pattern when: I) the induction zone is much less than the reaction zone; II) the induction zone behind the leading shock is much larger than the reaction zone.

Fig. 3 shows a typical flow structure of the self-sustaining detonation wave of type I. The dotted zone is that of energy release.

The flow pattern for the detonation with kinetic parameters of type II is quite different (Fig. 4): the flow is unstable with strong transverse pulsations. Those transverse pulsations originated in a symmetrical flow as a result of one-dimensional pulsations of the initial plane detonation wave in the bounded channel.

6. Experimental results.

Experimental investigations of deflagration to detonation transition in a bounded channel of a square cross-section 25 × 25 mm in a hydrocarbon air mixture were carried out. Visualisation of the flow was performed by the schlieren method with the help of a laser source of light.

At the final stage of the transition section (L = 1690 mm), different cases of combustion-to-detonation transition take place. Figs. 5–9 illustrate different types of flow patterns in the optical sections. The following nomenclature is used in the figures: 1,2,3 – primary shock waves; 4 – compression waves; 5 – flame zone; 6 – detonation wave; 7 – retonation wave; 8 – waves originating as a result of reflection of the detonation wave from walls of the tube; 9 – contact surfaces originating as a result of

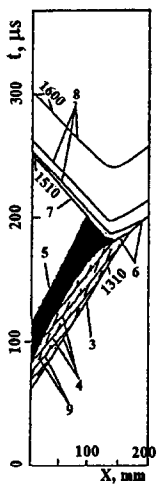

Fig. 5. Combustion to detonation transition. Origination of the detonation wave in the flame zone.

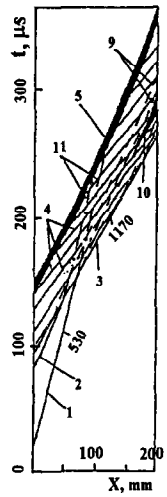

Fig. 6. Origination of spontaneous ignition between the flame zone and the shock wave on the contact surface after the interaction of two primary shock waves.

shock wave interactions, 10 – spontaneous flames, originating on the contact surfaces; 11 – first characteristics of rarefaction waves, originating as a result of shock wave interaction; velocities of waves in meters per second are printed on the figures parallel to the wave trajectories. Fig. 5 shows the case in which the primary shock wave and flame complex spread through the undisturbed mixture. Detonation occurs on the flame front immediately.

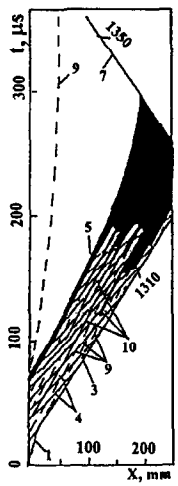

Fig. 7. Spontaneous ignition of gas in front of the flame zone and the shock wave on the contact surfaces that causes the detonation wave (not presented in the picture) and the retonation wave 7.

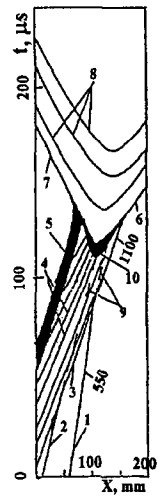

Fig. 8. Combustion to detonation transition $x-t$ diagram. Origination of the spontaneous flame and detonation wave on the contact surface between primary shock and the flame zone.

It is shown experimentally that several types of transition processes are possible. The first type: the detonation wave originates in the flame zone, accelerates rapidly and after the interaction with the leading shock forms a strong detonation wave that slows down to the Chapman–Jouget regime (Fig. 5). The second type: the detonation originates on the contact surface located in the zone between the leading shock and the flame (Fig. 9). This local explosion gives birth to the detonation and retonation waves. The third type: ignition takes place on the contact surface between the flame zone and the leading

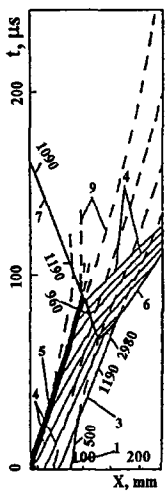

Fig. 9. Combustion to detonation transitiion $x-t$ diagram. Origination of the detonation wave on the contact surface between the flame zone and the primary shock wave.

shock. Turbulent combustion leads to the origin of detonation and retonation waves (Figs. 6 and 8). The fourth type: ignition takes place in several places in front of the flame zone very rapidly and causes the origination of the detonation wave. The flow pattern is similar to volumetric explosion or spontaneous flame (Fig. 7).

7. Reflection of deflagration and detonation waves

The problem of reflection of waves from the walls in combustion in bounded volumes is very important for determining the rates of dynamical wall loadings.

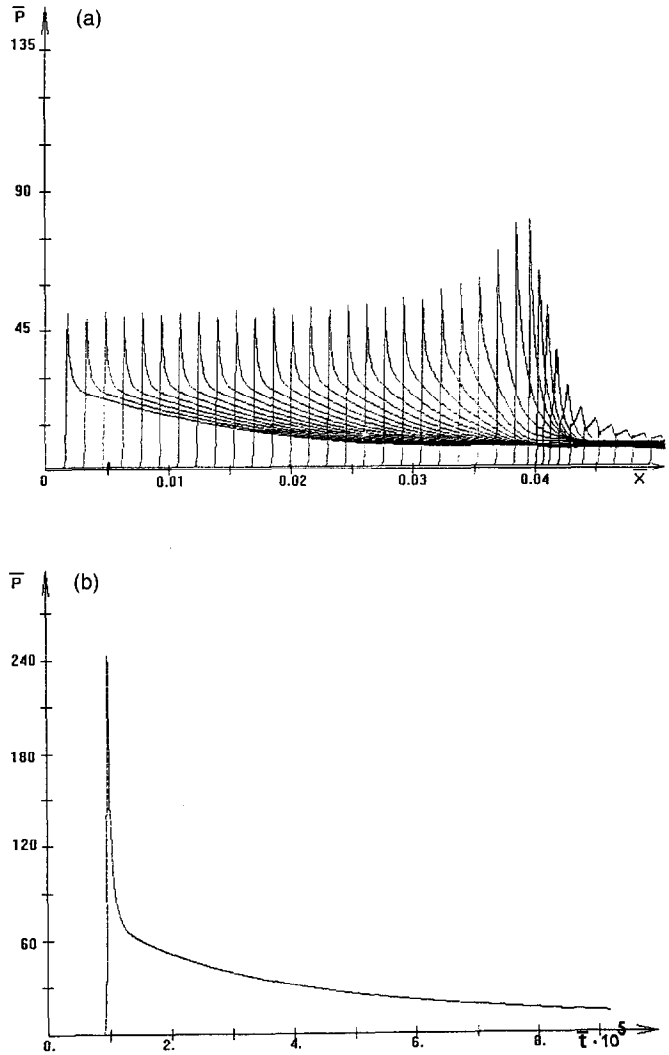

Fig. 10. The evolution of pressure profiles in the DDT process (a) and the pressure–time diagram for wall loading in reflected detonation wave (b).

Dynamical loadings are responsible for wall destructions and break-ups ofvessels in accidental ignitions of combustible mixtures. It is known that the criteria of destruction of vessels under dynamical loadings are different from that under the influence of static overpressure. More precise information about the rates of wall loadings in combustion in closed vessels is necessary to forecast the results of accident caused by unexpected ignition.

Theoretical and experimental investigations of the deflagration to detonation transition (DDT) following a soft ignition of a combustible mixture presented in this paper

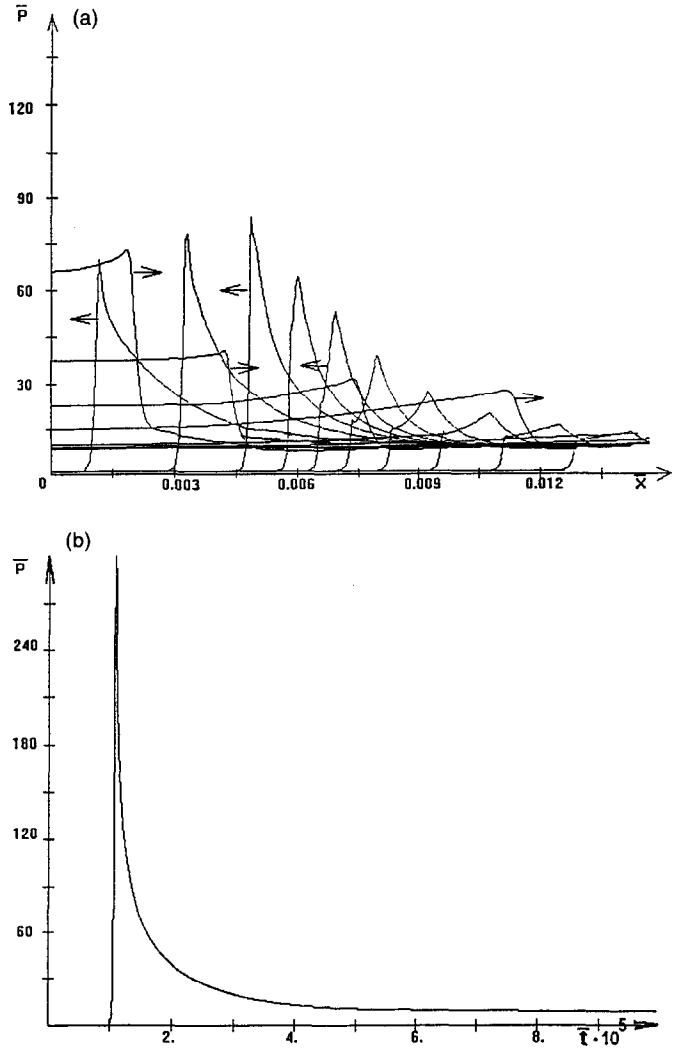

Fig. 11. Pressure profiles (a) and wall pressure (b) in reflection of unsteady decelerating detonation wave after the DDT.

show the process has several distinct scenarios. It is thus necessary to investigate the wall loadings resulting from the reflected waves born in the deflagration to detonation transition process at different stages of its development.

Let us regard theoretically the reflection of detonation and deflagration waves at different stages of the DDT process from a flat noncatalytic wall. The worked out numerical model will be used for this purpose.

Fig. 10(a) shows the time evolution of pressure profiles for the DDT-process in 1D calculations. The ignition took place on the right side and waves propagate from the right to the left. It is seen that the amplitudes of the waves are rather low near the

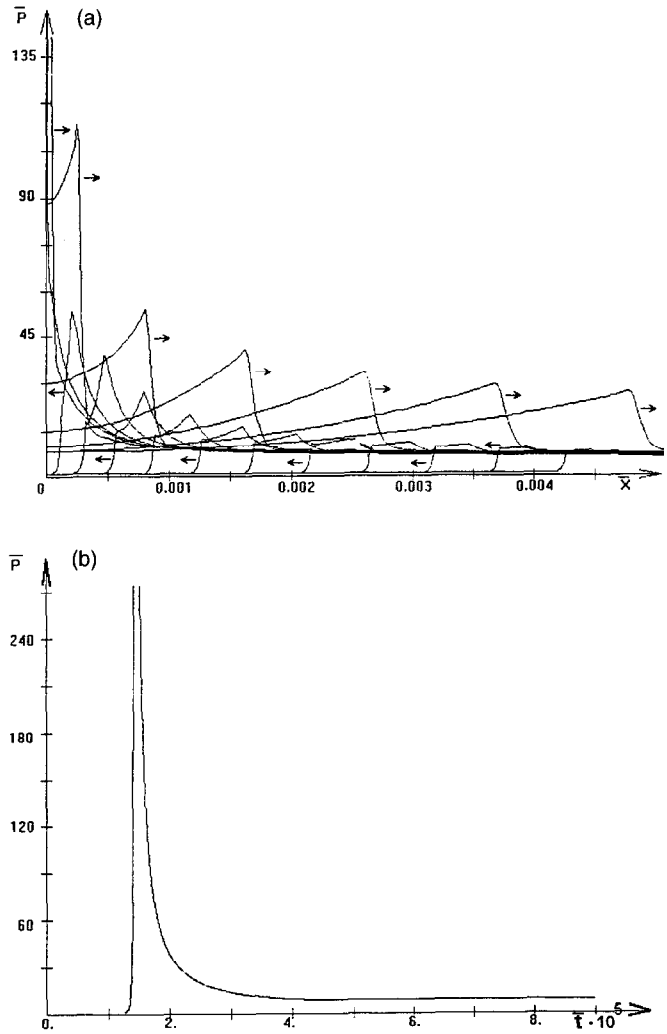

Fig. 12. Pressure profiles (a) and wall pressure evolution (b) in reflection of an overdriven detonation wave born in the DDT process.

ignition zone where deflagration and leading shockwaves propagate separately. Then the amplitudes increase essentially for overdriven detonation waves in the DDT-zone and then decrease to the values of a self-sustaining detonation with slight pulsations near the equilibrium caused by the instability of a plane detonation wave. We shall examine the rates of wall loadings at different stages of the DDT-process.

Fig. 10(b) shows the pressure–time diagram of wall loading in a reflected detonation wave. To characterise the wall loading we can introduce a value $I=(1/t^*)\int_0^{t^*} p\,dt$, a mean impulse over time interval $t\in[t_0,t_0+t^*]$, where t^* is a characteristic time. In

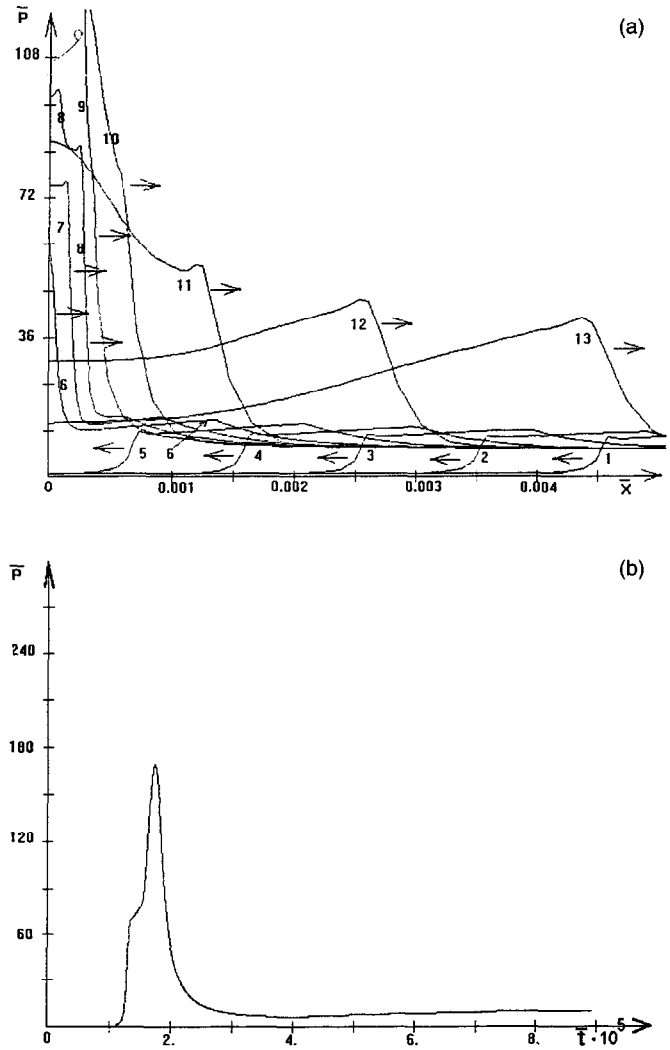

Fig. 13. Pressure profiles (a) and wall pressure evolution (b) in reflection of shock wave supported by accelerating flame zone when secondary ignition takes place near the wall behind the reflected shock wave.

our calculations this value can be chosen arbitrarily, but in fact it is connected with the characteristic time of wall response to loading. The evolution of a dimensionless mean impulse with the increase of characteristic time for this case is shown in Fig. 14, curve 1. Mean impulse $\bar{I}$ decreases with the increase of characteristic time.

Fig. 11(a) and (b) show pressure profiles and pressure–time diagram, respectively, for the case in which reflection takes place just after the transition. It is seen that maximal pressures in the reflected wave are higher than those in the previous case.

The mean impulse $\bar{I}$ for this case (curve 2 in Fig. 14) is higher for short characteristic times ($\bar{T}^* < 2 \times 10^{-5}$) and lower for longer times than that for the first case (curve 1 in Fig. 14).

Fig. 12 corresponds to the case of an overdriven detonation wave reflection and manifests even higher values of pressure and impulse for short characteristic times (compare curve in Fig. 14).

Fig. 13 shows the reflection process when the distance to the wall was too short for the DDT. A compression wave followed by a deflagration wave reflects from the wall. At the first instant the pressure growth in the reflected shockwave is not too high as compared with the previous case. But later chemical reactions start near the wall in the gas compressed by the reflected shockwave (curves 8, 9, 10 in Fig. 13(a)). This gives birth to a secondary growth of wall pressure (Fig. 13(b)) and increases the mean impulse (curve 4 in Fig. 14).

Fig. 14 shows the time evolution of the mean impulse $\bar{I}$ for the regarded reflections. It can be seen that even for the last case of reflection wherein the detonation wave was not formed (curve 4), there exist characteristic times corresponding to a mean impulse higher than that in the reflection of a normal detonation wave (curve 1).

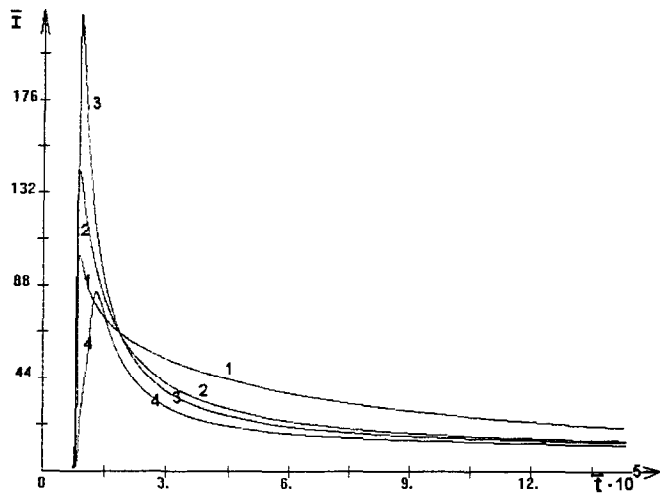

Fig. 14. Evolution of mean impulse of wall loading $\bar{I} = (1/t^*)\int_0^{t^*} \bar{p}\,dt$ in reflection of detonation waves at different stages of the DDT: curve 1 corresponds to the case shown in Fig. 10; curve 2 – Fig. 11; curve 3 – Fig. 12; curve 4 – Fig. 13.

For the case of a slow deflagration wave when the DDT-process does not take place, the rate of pressure growth on the wall is much lower and the maximal amplitude corresponds to the equilibrium pressure that can be estimated by a formula:

$$\frac{p_2}{p_1} = \gamma\bar{p} = \frac{\gamma_2 - 1}{\gamma_1 - 1}\left(1 + \gamma_1 \frac{\Delta H}{c_{p1}T_1}\right). \tag{12}$$

For the case examined, this value is of the order of ten.

These investigations of internal mechanisms of gaseous explosions are very important for determining the rates of wall loadings.

8. Conclusions

A mathematical model and algorithm for the simulation of the initiation of combustion and detonation in a viscous heat-conductive reactive mixture is constructed, wherein the chemistry is modelled by a two-step chemical reaction.

Experimental investigations of the deflagration to detonation transition showed four possible mechanisms of the process.

Numerical simulations show as well that an acceleration of the reaction zone preceded by several shock waves can be a result of the interaction of the contact surface with the flame zone overtaking it.

An investigation of two-dimensional detonation waves in the layers of detonable mixtures with free boundaries shows that the curvature of the leading shock wave due to expansion of the reaction products leads to the formation of a transsonic flow behind the shock wave. The energy release takes place in both subsonic and supersonic zones. The leading shock is sustained not only by the energy release in the subsonic zone but also by that from a definite part of a supersonic zone bounded by characteristics. On increasing the length of the induction zone the flow field becomes unstable. There occur strong transverse pulsations of the leading shock. On decreasing the length of the induction zone the amplitude of pulsations decreases and they become indistinguishable within the frames of numerical resolution.

Rates of wall loadings in reflected detonation and deflagration waves and mean impulses necessary to estimate the explosion's hazards to the surrounding structures were investigated. It was shown that the rates of loading, the maximal pressure in the reflected wave and the mean impulse for short characteristic times are highest for the case of a reflection of an overdriven detonation wave appearing in the deflagration to detonation transition process.[17]

Acknowledgements

We gratefully acknowledge the financial support of the Russian Basic Research Foundation (Project Codes 94-03-08613 and 96-03-32002).

References

[1] A.K. Oppenheim and R.I. Soloukhin, Ann. Rev. Fluid Mech. 5 (1973) 31.
[2] G.D. Salamandra et al., Some methods of exploration of quick-going processes and their application to the investigation of forming a detonation wave (Izdatelstvo Akademii Nauk SSSR, Moscow, 1960).
[3] R.I. Soloukhin, Methods of measure and main results of experiments in shock tubes (Izdatelstvo Novosibirskogo Universiteta, Novosibirsk, 1969).
[4] J.F. Clarke and N. Riley, J. Fluid. Mech. 167 (1986) 409.
[5] Ya.B. Zeldovich, V.B. Librovich, G.M. Makhviladze and G.I. Sivashinsky, Prikladnaya Mechanika i Technicheskaya Fizika, N 2 (1970) 76.
[6] B.E. Gelfand, G.M. Makhviladze, D.I. Rogatykh and S.M. Frolov, Spontaneous forming of explosive regimes of reaction in the regions with non-uniformities of temperature and concentration. Preprint N 358 (Institut Problem Mekhaniki Akademii Nauk SSSR, Moscow, 1988).
[7] B.E. Gelfand, S.M. Frolov, A.N. Polenov and S.A. Tsyganov, Himicheskaya Fizika 5, N 9 (1986) 1277.
[8] J.F. Clarke, D.R. Kassoy and N. Riley, Proc. R. Soc. (London) A 408 (1986) 129.
[9] N.N. Smirnov, An.Yu. Demyanov and I.I. Panfilov, Himicheskaya Fizika processov goreniya i vzryva. Detonatsya. Materialy IX Vsesoyuznogo Sympoziuma po Goreniyu i vzryvu. (Izdatelstvo Akademii Nauk SSSR, Chernogolovka, 1989), pp. 52–56.
[10] P.A. Urtiew and A.K. Oppenheim, Proc. R. Soc. (London) A 295 (1966) 13.
[11] P.A. Urtiew and A.K. Oppenheim, Proc. R. Soc. (London) A 304 (1968) 379.
[12] P. Wolanski, Archivum Combustionis, Vol.11, No.3, 4 (1991) 143.
[13] Yu.A. Demyanov, G.V. Sekrieru, A.I. Igoshin, V.T. Kireev and V.L. Pinsky, One-dimensional flows of real gas (Shtinitsa, Kishinev, 1980).
[14] E.S. Oran and J.P. Boris, Progress Energy Combustion Science 7 (1981) 1.
[15] N.N. Smirnov, I.I. Panfilov, Deflagration to detonation transition as a source of noise in automobile engines, Proc. International Sci. Conf. on Internal Combustion Engines, KONES'93, GDANSK – JURATA, September 1993, pp. 545–552.
[16] N.N. Yanenko, Split step method of solution of multidimension problems of mathematical physics (Nauka, Novosibirsk, 1967).
[17] V.P. Korobeinikov, Problems of Point-Blast Theory (American Institute of Physics, New York, 1991), p. 382 [English translation].